

1 **The pCO₂ estimates of the late Eocene in South China based on**
2 **stomatal density of *Nageia Gaertner* leaves**

3
4 XIAO-YAN LIU, QI GAO, MENG HAN and JIAN-HUA JIN*

5
6 State Key Laboratory of Biocontrol and Guangdong Provincial Key Laboratory of Plant Resources,
7 School of Life Sciences, Sun Yat-sen University, Guangzhou 510275, China

8
9 **Abstract:**

10 Atmospheric pCO₂ concentrations have been estimated for intervals of the Eocene
11 using various models and proxy information. Here we reconstruct late Eocene (~ 40.3
12 Ma) pCO₂ based on the fossil leaves of *Nageia maomingensis* Jin et Liu collected
13 from the Maoming Basin, Guangdong Province, China. We first determine
14 relationships between atmospheric pCO₂ concentrations, stomatal density (SD) and
15 stomatal index (SI) using “modern” leaves of *N. motleyi* (Parl.) De Laub, the nearest
16 living species to the Eocene fossils. This work indicates that the SD inversely
17 responds to pCO₂, while SI has almost no relationship with pCO₂. Eocene pCO₂
18 concentrations can be reconstructed based on a regression approach and the stomatal
19 ratio method by using the SD. The first approach gives a pCO₂ of 351.9 ± 6.6 ppmv,
20 whereas the one based on stomatal ratio gives a pCO₂ of 537.5 ± 56.5 ppmv. Here, we
21 explored the potential of *N. maomingensis* in pCO₂ reconstruction and obtained

*

Correspondence: Jianhua Jin, tel. +86 20 84113348, fax +86 20 84110436, e-mail: lssjhh@mail.sysu.edu.cn

22 different results according to different methods, providing a new insight for the
23 reconstruction of paleoclimate and paleoenvironment in conifers.

24

25 **Keywords:** pCO₂, late Eocene, *Nageia*, Maoming Basin, South China.

26

27 **1 Introduction**

28

29 The Eocene (55.8-33.9 Ma) generally was much warmer than present-day, although
30 temperatures varied significantly across this time interval (Zachos et al., 2008).

31 Climate of the early Eocene was extremely warm, particularly during the early
32 Eocene Climatic Optimum (EECO; 51 to 53 Ma), and the Paleocene-Eocene Thermal
33 Maximum (PETM; ~55.9 Ma). However, global climatic conditions cooled
34 significantly by the late Eocene (40 to 36 Ma). Indeed, small, ephemeral ice-sheets
35 and Arctic sea ice likely existed during the latest Eocene (Moran et al., 2006; Zachos
36 et al., 2008).

37 Many authors have suggested that changes in temperature during the Phanerozoic
38 were linked to atmospheric pCO₂ (Petit et al., 1999; Retallack, 2001; Royer, 2006).
39 Central to these discussions are records across the Eocene, as this epoch spans the last
40 major change from a “greenhouse” world to an “icehouse” world. The Eocene pCO₂
41 record remains incomplete and debated (Kürschner et al., 2001; Royer et al., 2001;
42 Beerling et al., 2002; Greenwood et al., 2003; Royer, 2003). Most pCO₂
43 reconstructions have focused on the Cretaceous-Tertiary and Paleocene-Eocene

44 boundaries (65 to 50 Ma; Koch et al., 1992; Stott, 1992; Sinha and Stott, 1994; Royer
45 et al., 2001; Beerling and Royer, 2002; Nordt et al., 2002; Royer, 2003; Fletcher et al.,
46 2008; Roth-Nebelsick et al., 2012; 2014; Grein et al., 2013; Huang et al., 2013;
47 Maxbauer et al., 2014) and the middle Eocene (Maxbauer et al., 2014), while few
48 reconstructions were conducted at the late Eocene. In addition, the pCO₂
49 reconstruction results have varied based on different proxies. Various methods having
50 been used in pCO₂ reconstruction mainly include the computer modeling methods:
51 GEOCARB-I, GEOCARB-II, GEOCARB-III, GEOCARB-SULF and the proxies: ice
52 cores, paleosol carbonate, phytoplankton, nahcolite, Boron, and stomata parameters.

53 The abundance of stomatal cells can be measured on modern leaves and
54 well-preserved fossil leaves. Various plants show a negative correlation between
55 atmospheric CO₂ concentration and stomatal density (SD), stomatal index (SI), or
56 both. As such, these parameters have been determined in fossil leaves to reconstruct
57 past pCO₂; examples include *Ginkgo* (Retallack, 2001, 2009a; Beerling et al., 2002;
58 Royer, 2003; Kürschner et al., 2008; Smith et al., 2010), *Metasequoia* (Royer, 2003;
59 Doria et al., 2011), *Taxodium* (Stults et al., 2011), *Betula* (Kürschner et al., 2001; Sun
60 et al., 2012), *Neolitsea* (Greenwood et al., 2003), and *Quercus* (Kürschner et al., 1996,
61 2001), *Laurus* and *Ocotea* (Kürschner et al., 2008). Recently, positive correlations
62 between stomatal index or stomatal frequency and pCO₂ have been reported based on
63 fossil *Typha* and *Quercus* (Bai et al., 2015; Hu et al., 2015). However, the tropical and
64 subtropical moist broadleaf forest conifer tree *Nageia* has not been used previously in
65 paleobotanical estimates of pCO₂ concentration.

66 Herein, we firstly document correlations between stomatal properties and
67 atmospheric CO₂ concentrations using leaves of the extant species *Nageia motleyi*
68 (Parl.) De Laub. that were collected over the last two centuries. This provides a
69 training dataset for application to fossil representatives of *Nageia*. We secondly
70 measure stomatal parameters on fossil *Nageia* leaves from the late Eocene of South
71 China to estimate past CO₂ levels. The work provides further insights for discussing
72 Eocene climate change.

73

74 **2 Background**

75

76 **2.1 Stomatal proxy in pCO₂ research**

77

78 Stomatal information gathered from careful examination of leaves has been widely
79 used for reconstructions of past pCO₂ concentrations (Beerling and Kelly, 1997; Doria
80 et al., 2011). The three main parameters are stomatal density (SD), which is expressed
81 as the total number of stomata divided by area, epidermal density (ED), which is
82 expressed as the total number of epidermal cells per area, and the stomatal index (SI),
83 which is defined as the percentage of stomata among the total number of cells within
84 an area [$SI = SD \times 100 / (SD + ED)$]. Woodward (1987) considered that both SD and SI
85 had inverse relationships with atmospheric CO₂ during the development of the leaves.
86 Subsequently, McElwain (1998) created the stomatal ratio (SR) method to reconstruct
87 pCO₂. SR is a ratio of the stomatal density or index of a fossil [$SD_{(f)}$ or $SI_{(f)}$] to that of

88 corresponding nearest living equivalent [$SD_{(e)}$ or $SI_{(e)}$], expressed as follows:

$$89 \quad SR = SI_{(e)} / SI_{(f)} \quad (1)$$

90 The stomatal ratio method is a semi-quantitative method of reconstructing pCO₂
91 concentrations under certain standardizations. An example is the “Carboniferous
92 standardization” (Chaloner and McElwain, 1997), where one stomatal ratio unit
93 equals two RCO₂ units:

$$94 \quad SR = 2 \text{ RCO}_2 \quad (2)$$

95 and the value of RCO₂ is the pCO₂ level divided by the pre-industrial atmospheric
96 level (PIL) of 300 ppm (McElwain, 1998) or that of the year when the nearest living
97 equivalent (NLE) was collected (Berner, 1994; McElwain, 1998):

$$98 \quad \text{RCO}_2 = C_{(f)} / 300 \text{ or } \text{RCO}_2 = C_{(f)} / C_{(e)} \quad (3)$$

99 The estimated pCO₂ level can then be expressed as follows:

$$100 \quad C_{(f)} = 0.5 \times C_{(e)} \times SD_{(e)} / SD_{(f)} \text{ or } C_{(f)} = 0.5 \times C_{(e)} \times SI_{(e)} / SI_{(f)} \quad (4)$$

101 where $C_{(f)}$ is the pCO₂ represented by the fossil leaf, and $C_{(e)}$ is the atmospheric CO₂
102 of the year when the leaf of the NLE species was collected (McElwain and Chaloner,
103 1995, 1996; McElwain 1998). The equation adapts to the pCO₂ concentration prior to
104 Cenozoic.

105 Another standardization, the “Recent standardization” (McElwain, 1998), is
106 expressed as one stomatal ratio unit being equal to one RCO₂ unit:

$$107 \quad SR = 1 \text{ RCO}_2 \quad (5)$$

108 According to the equations stated above, the pCO₂ concentration can be expressed
109 as:

110 $C_{(f)} = C_e \times SD_{(e)} / SD_{(f)}$ or $C_{(f)} = C_e \times SI_{(e)} / SI_{(f)}$ (6)

111 This standardization is usually used for reconstruction based on Cenozoic fossils
112 (Chaloner and McElwain, 1997; McElwain, 1998; Beerling and Royer, 2002).

113 Kouwenberg et al. (2003) proposed some special stomatal quantification methods
114 for conifer leaves with stomata arranged in rows. The stomatal number per Length
115 (SNL) is expressed as the number of abaxial stomata plus the number of adaxial
116 stomata divided by leaf length in millimeters. Stomatal rows (SRO) is expressed as
117 the number of stomatal rows in both stomatal bands. Stomatal density per length
118 (SDL) is expressed as the equation $SDL = SD \times SRO$. True stomatal density per
119 length (TSDL) is expressed as the equation $TSDL = SD \times \text{band width (in millimeters)}$.
120 The band width on *Nageia motleyi* leaves was measured as leaf blade width.

121

122 **2.2 Review of extant and fossil *Nageia***

123

124 The genus *Nageia*, including seven living species, is a special group of
125 Podocarpaceae, a large family of conifers mainly distributed in the southern
126 hemisphere. *Nageia* has broadly ovate-elliptic to oblong-lanceolate, multiveined
127 (without a midvein), spirally arranged or in decussate, and opposite or subopposite
128 leaves (Cheng et al., 1978; Fu et al., 1999). Generally, *Nageia* is divided into *Nageia*
129 Sect. *Nageia* and *Nageia* Sect. *Dammaroideae* (Mill 1999, 2001). Both sections are
130 mainly distributed in southeast Asia and Australasia from north latitude 30 ° to nearly
131 the equator (Fu, 1992; Fig. 1). Four species of the *N.* section *Nageia* -- *Nageia nagi*

132 (Thunberg) O. Kuntze, *N. fleuryi* (Hickel) De Laub., *N. formosensis* (Dummer) C. N.
133 Page, and *N. nankoensis* (Hayata) R. R. Mill -- have hypostomatic leaves where
134 stomata only occur on the abaxial side. One species of this section -- *N. maxima* (De
135 Laub.) De Laub. -- is characterized by amphistomatic leaves, but where only a few
136 stomata are found on the adaxial side (Hill and Pole, 1992; Sun, 2008). Both *N.*
137 *wallichiana* (Presl) O. Kuntze and *N. motleyi* of the *N.* section *Dammaroideae* are
138 amphistomatic with abundant stomata distributed on both sides of the leaf. This is
139 especially true for *N. motleyi*, which has approximately equal stomata numbers on
140 both surfaces (Hill and Pole, 1992; Sun, 2008).

141 The fossil record of *Nageia* can be traced back to the Cretaceous. Krassilov (1965)
142 described *Podocarpus (Nageia) suifunensis* Krassilov from the Lower Cretaceous of
143 Far East Russia. Kimura et al. (1988) reported *Podocarpus (Nageia) ryosekiensis*
144 Kimura, Ohanaet Mimoto, an ultimate leafy branch bearing a seed, from the Early
145 Barremian in southwestern Japan. In China, a Cretaceous petrified wood, *Podocarpus*
146 (*Nageia*) *nagi* Pilger, was discovered from the Dabie Mountains in central Henan,
147 China (Yang et al., 1990). Jin et al. (2010) reported a upper Eocene *Nageia* leaf
148 named *N. hainanensis* Jin, Qiu, Zhu et Kodrul from the Changchang Basin of Hainan
149 Island, South China. Recently, Liu et al. (2015) found another leaf species *N.*
150 *maomingensis* Jin et Liu from upper Eocene of Maoming Basin, South China.
151 Although some of the *Nageia* fossil materials described in the above studies
152 (Krassilov, 1965; Jin et al., 2010; Liu et al., 2015) have well-preserved cuticles, these
153 studies are mainly concentrated on morphology, systematics and phytogeography.

154 Here we try to reconstruct the pCO₂ concentration based on stomatal data of
155 *Nageia maomingensis* Jin et Liu. Among the modern *Nageia* species mentioned above,
156 *N. motleyi* was considered as the NLE species of *N. maomingensis* (Liu et al., 2015).
157 However, because of the species-specific inverse relationship between atmospheric
158 CO₂ partial pressure and SD (Woodward and Bazzaz, 1988), it is necessary to explore
159 whether the SD and SI of *N. motleyi* show negative correlations with the CO₂
160 concentration before applying the stomatal method. Both *N. maomingensis* and *N.*
161 *motleyi* are amphistomatic, suggesting that both upper and lower surfaces of the leaf
162 are needed to estimate the pCO₂ concentrations.

163

164 **3 Material and methods**

165

166 **3.1 Extant leaf preparation**

167

168 We examined 12 specimens of extant *Nageia motleyi* from different herbaria (Table
169 1). We removed one or two leaves from each specimen, and took three fragments
170 (0.25 mm²) from every leaf (Fig. 2a) and numbered them for analysis.

171 The numbered fragments were boiled for 5-10 min in water. Subsequently, after
172 being macerated in a mixed solution of 10% acetic acid and 10% H₂O₂ (1:1) and
173 heated in the thermostatic water bath at 85 C for 8.5 hours; the reaction was stopped
174 when the specimens fragments turned white and semitransparent; The cuticles were
175 then rinsed with distilled water until the pH of the water became neutral. After that the

176 cuticles were treated in Schulze's solution (one part of potassium chlorate saturated
177 solution and three part of concentrated nitric acid) for 30 min, rinsed in water, and
178 then treated with 8% KOH (up to 30 min) and the abaxial and adaxial cuticles were
179 separated with a hair mounted on needle. Finally, the cuticles were stained with 1%
180 Safranin T alcoholic solution for 5 min, sealed with Neutral Balsam and observed
181 under LM.

182

183 **3.2 Fossil leaf preparation**

184

185 Maoming Basin (21°42'33.2"N, 110°53'19.4"E) is located in southwestern
186 Guangdong, South China including Cretaceous and Tertiary strata. Tertiary strata are
187 fluvial and lacustrine sedimentary units, divided into the Gaopengling, Laohuling,
188 Shangcun, Huangniuling and Youganwo formations in descending order, aged from
189 late Eocene to early Oligocene (Wang et al., 1994).

190 Four fossil leaves of *Nageia maomingensis* were recovered from the Youganwo
191 (MMJ1-001) and Huangniuling (MMJ2-003, MMJ2-004 and MMJ3-003) formations
192 of Maoming Basin, South China (Fig. 1B, 1C in Liu et al., 2015). The age from
193 Youganwo to Huangniuling formations is late Eocene (~ 40.3 Ma). Precise
194 information regarding locations is provided by Liu et al., (2015). Macrofossil
195 cuticular fragments were taken from the middle part of each fossil leaf (Fig. 2c) and
196 treated with Schulze's solution for approximately 1h and 5–10% KOH for 30 min (Ye,
197 1981). The cuticles were observed and photographed under a Carl Zeiss Axio Scope

198 A1 light microscope (LM). All fossil specimens and cuticle slides are housed in the
199 Museum of Biology of Sun Yat-sen University, Guangzhou, China.

200

201 **3.3 Stomatal counting strategy and calculation methods**

202

203 The basic stomatal parameters, SD, ED and SI, were counted based on analyzing
204 pictures taken with a light microscope (LM). A total of 2816 pictures (200×
205 magnification of Zeiss LM) of cuticles from 21 leaves of *N. motleyi* were counted.
206 Each counting field was 0.366 mm². We used a standard sampling protocol (Poole and
207 Kürschner, 1999), counting all full stomata in the image plus stomata straddling the
208 left and top margins, as presented in Figure 2(b), and (d).

209 The SNL, SRO, SDL, and TSDL were also determined based on LM images. A
210 total of 2293 pictures (200× magnification of Zeiss LM) of the cuticles from 21 leaves
211 of *N. motleyi* were counted. Each counting field was 0.366 mm². None of the
212 aforementioned counting areas overlapped and they were larger than the minimum
213 area (0.03 mm²) for statistics (Poole and Kürschner, 1999). In this study, the stomatal
214 data of both surfaces are applied in pCO₂ reconstruction because both the fossil and
215 NLE species are amphistomatic.

216

217

218 **4 Results**

219

220 **4.1 Correlations between the CO₂ concentrations and stomatal parameters of**
221 *Nageia motleyi*

222

223 The SD and SI data of the adaxial sides of *N. motleyi* leaves are presented in Table
224 2. The SDs and SIs average 62.28 mm⁻² and 3.30 %, respectively. However, the SDs
225 and SIs data of the abaxial sides, summarized in Table 3, give higher average values
226 (70.03 mm⁻² in SDs and 3.90 % in SIs) than those from the adaxial sides. The
227 combined SD and SI of the adaxial and abaxial surfaces average 66.14 mm⁻² and
228 3.60 %, respectively (table 4).

229 Fig. 3 shows the relationships between the stomatal parameters (SD and SI) of
230 modern *N. motleyi* and the atmospheric CO₂ concentration (SD-CO₂ relationship and
231 SI-CO₂ relationship). R² values in the SD-CO₂ relationship from the adaxial and
232 abaxial surfaces of *N. motleyi* are up to 0.4667 and 0.3824 (Fig. 3a, b), suggesting that
233 the stomatal densities of *N. motleyi* are inverse to the CO₂ concentrations. However,
234 Fig. 3c and d indicate no relationship between the SIs and CO₂ concentrations for the
235 extremely low level of the R² values (0.2558 and 0.0248). Figs. 3e and 3f based on the
236 combined data also show that SD inversely responds to the atmospheric CO₂
237 concentration (R² =0.4421), while SI has almost no relationship with the atmospheric
238 CO₂ concentration (R² =0.1177).

239 The mean values of SNL, SDL and TSDL are 9.81, 326.39 and 1226.93 no.·mm⁻¹,
240 respectively (Table 5). Fig. 4 shows the relationships between SNL (SDL, TSDL) and
241 CO₂ concentrations. The low R² values in the Fig. 4a and 4c indicate that SNL (R² =

242 0.0643) and TSDL ($R^2 = 0.0788$) have no relationship with the CO₂ concentration in
243 this study. Fig. 4b shows that there is a weak reverse relevance between SDL and the
244 CO₂ concentration ($R^2 = 0.3154$).

245 Compared with the SDL method, the SD-based method shows a larger R^2 value,
246 indicating a stronger relevance between the SD and CO₂ concentrations. In this study,
247 the pCO₂ is reconstructed based on the regression equations of SD-CO₂ relationship.
248 Additionally, the stomatal ratio method can be also used in estimating pCO₂
249 concentration of the late Eocene based on stomatal densities (SDs) of the fossil
250 species *N. maomingensis* and extant species *N. motleyi*. The SD results of specimen
251 No. 18328 are selected to reconstruct the pCO₂ concentration, because they are closest
252 to the fitted equations in Fig. 3. This specimen was collected by Neth. Ind. For.
253 Service from Riau on Ond. Karimon, Archipel. Ind., Malaysia, in 1934 at an altitude
254 of 5 m and CO₂ concentration of 306.46 ppmv (Brown, 2010).

255

256 **4.2 The pCO₂ estimates results**

257 4.2.1 The regression approach

258 The summary of stomatal parameters of the fossil *Nageia* and reconstruction results
259 are provided in Tables 6–8. The mean SD and SI values of the adaxial surface are 44.5
260 mm⁻² and 1.8 %, respectively (Table 6). The mean SD and SI values of the abaxial
261 surface are 49.8 mm⁻² and 2.07 %, respectively (Table 7).

262 Based on the regression approach, the pCO₂ was reconstructed as 351.9 ± 6.6 ppmv
263 and 365.6 ± 7.6 ppmv according to the SD of adaxial and abaxial sides. The combined

264 SD value is an average of 46.6 mm^{-2} (Table 8), giving the reconstructed pCO_2 of
265 358.1 ± 5.0 ppmv.

266

267 4.2.2 The stomatal ratio method

268 Mean SR value of the adaxial side ($\text{SR}=1.69 \pm 0.18$) is a little larger than that of the
269 abaxial side ($\text{SR}=1.60 \pm 0.11$) in fossil *Nageia* leaves (Tables 6 and 7). The pCO_2
270 reconstruction results are 537.5 ± 56.5 ppmv (Table 6) and 496.1 ± 35.7 ppmv (Table 7)
271 based on the adaxial and abaxial cuticles, respectively. Based on the combined SD of
272 both leaf sides, the pCO_2 result is 519.9 ± 35.0 ppmv.

273 The partial pressure of CO_2 decreases with elevation (Gale, 1972). Jones (1992)
274 proposed that the relationship between elevation and partial pressure in the lower
275 atmosphere can be expressed as $P = -10.6E + 100$, where E is elevation in kilometers
276 and P is the percentage of partial pressure relative to sea level. Various studies
277 corroborate that SI and SD of many plants have positive correlations with altitude
278 (Körner and Cochrane, 1985; Woodward, 1986; Woodward and Bazzaz, 1988;
279 Beerling et al., 1992; Rundgren and Beerling, 1999) while they are negatively related
280 to the partial pressure of CO_2 (Woodward and Bazzaz, 1988). Therefore, it is essential
281 to take elevation calibration into account during pCO_2 concentration estimates.
282 However, Royer (2003) pointed out that it is unnecessary to provide this conversion
283 when trees lived at <250 m in elevation. In this paper, the nearest living equivalent
284 species, *Nageia motleyi*, grows at 5 m in elevation with $P = 99.9$, suggesting that CO_2
285 concentration estimates were only underestimated by 0.1%. Consequently, no

286 correction is needed for the reconstruction result in this study. After being projected
287 into a long-term carbon cycle model (GEOCARB III; Berner and Kothavala 2001),
288 the results of this study compares well with CO₂ concentrations for corresponding age
289 within their error ranges (Fig. 5).

290

291 **5 Discussion**

292 **5.1 Stomatal parameters response to CO₂**

293 Here, we find that SD decreases as atmospheric CO₂ concentrations increase,
294 however, SI does not. Generally, SI is more sensitive in response to the atmospheric
295 CO₂ concentration than SD (Beerling, 1999; Royer, 2001). However, the reverse case
296 is not unfound. For example, Kouwenberg et al. (2003) reported that SD is better than
297 SI in reflecting the negative relationships with CO₂ in conifer needles, accounting for
298 the special paralleled mode of the ordinary epidermal and stomatal formation.

299 Although *Nageia* is broad-leaved rather than needle-leaved, it also has well paralleled
300 epidermal cells herein showing the different relationships between CO₂ and SD or SI.
301 Compared with SD, the SDL has weaker correlation with CO₂ at a smaller R². The
302 SNL and TSDL have no response to the change of CO₂. The insensitivity of SNL,
303 SDL and TSDL might account for the characters of broad-leaved leaf shape and
304 paralleled epidermal cells. The SNL should be applied to conifer needles with single
305 file of stomata (Kouwenberg et al., 2003). The SDL and TSDL were considered as the
306 most appropriate method when the stomatal rows grouped in bands in a hypo- or
307 amphistomatal conifer needle species (Kouwenberg et al., 2003). Considering all the

308 stomatal parameters above, SD appears to be the most sensitive to CO₂.

309 The SD-CO₂ correlation shows one value from leaf No. 40798 offset from the
310 others. The SI-CO₂ correlation shows different offset values in different leaf sides.
311 The offset values might be affected by leaf maturity and light intensity. However, it is
312 hard to distinguish whether a fossil leaf is young or mature, or live in the sunny or
313 shady light regimes.

314 The R² value (0.5) of SD-CO₂ based on the adaxial side is higher than from the
315 abaxial side and the combination of both sides, indicating that the correlation of
316 SD-CO₂ is stronger than the others parameters herein. Therefore, the SD on the
317 adaxial side is the best in reconstructing pCO₂. The reconstruction result based on the
318 regression approach is 351.9 ± 6.6 ppmv lower than the one based on the stomatal
319 ratio method (Table 6), and it is relatively lower than the results based on the other
320 proxies (Fig. 6; Freeman and Hayes, 1992; Pagani et al., 2005; Maxbauer et al., 2014).
321 However, the result based on stomatal ratio method is 537.5 ± 56.5 ppmv which is
322 closest to GEOCARB III (Fig. 5) and historical reconstruction trends (Fig. 6).

323

324 **5.2 Paleoclimate reconstructed history**

325

326 The pCO₂ levels throughout the Cenozoic were relatively lower than through the
327 Cretaceous (Ekart et al., 1999), but had an overall decreasing trend with some
328 significant increases on short-time scales (e.g. in the earliest Eocene and middle
329 Miocene, Zachos et al., 2001, 2008; Wing et al., 2005; Lowenstein and Demicco,

330 2006; Fletcher et al., 2008; Bijl et al., 2010; Kato et al., 2011). There is a wide range
331 in pCO₂ estimates for the Paleogene, reflecting problems in the various proxies. Both
332 the fractionation of carbon isotopes by phytoplankton (Freeman and Hayes, 1992) and
333 analysis of paleosol (fossil soil) carbonates (Ekart et al., 1999) demonstrate that
334 carbon dioxide levels were less than 1000 ppmv before the Cretaceous-Tertiary
335 boundary and have been decreasing since the Paleocene.

336 Based on the measurements of palaeosol carbon isotopes, Cerling (1991) reported
337 that pCO₂ levels for the Eocene and Miocene through to the present was lower than
338 700 ppmv. Fletcher et al. (2008) also showed that atmospheric CO₂ levels were
339 approximately 680 ppmv by 60 million years ago. However, Stott (1992)
340 reconstructed pCO₂ as 450–550 ppmv for the early Eocene based on phytoplankton.
341 Additionally, reconstructions using the stomatal ratio method based on *Ginkgo*,
342 *Metasequoia*, and Lauraceae leaves also revealed a low pCO₂ level between 300 and
343 500 ppmv during the early Eocene (Kürschner et al., 2001; Royer et al., 2001;
344 Greenwood et al., 2003; Royer, 2003) except a single high estimate of about 800
345 ppmv near the Paleocene/Eocene boundary (Royer et al., 2001).

346 Subsequently, Smith et al. (2010) reconstructed the value of pCO₂ ranging from 580
347 ±40 to 780 ±50 ppmv using the stomatal ratio method (recent standardization) based
348 on both SI and SD. A climatic optimum occurred in the middle Eocene (MECO): the
349 reconstructed CO₂ concentrations are mainly between 700 and 1000 ppmv during the
350 late middle Eocene climate transition (42–38 Ma) using stomatal indices of fossil
351 *Metasequoia* needles, but concentrations declined to 450 ppmv toward the top of the

352 investigated section (Doria et al., 2011). Jacques et al. (2014) used CLAMP to
353 calibrate climate change in Antarctica during the early-middle Eocene, suggesting a
354 seasonal alternation of high- and low-pressure systems over Antarctica during the
355 early-middle Eocene. Spicer et al. (2014) also reconstructed a relatively lower cool
356 temperature than $\delta^{18}\text{O}$ records (Keating-Bitonti et al., 2011) in the middle Eocene of
357 Hainan Island, South China using CLAMP, indicating a not uniformly warm climate
358 in the low latitude during the Eocene. An overall decreasing trend of the pCO_2 level
359 was presented after the middle Eocene (Fig. 6; Retallack, 2009b).

360 The ice-sheets started to appear in the Antarctic during the Late Eocene (Zachos et
361 al., 2001), then the temperature suffered an apparent further decrease from the late
362 Eocene to the early Oligocene (Roth-Nebelsick et al., 2004), which resulted in the
363 Antarctic being almost fully covered by ice-sheets. Subsequently, the climate
364 variation was comparatively stable with a little wobbling in temperature during the
365 Oligocene period (Fig. 6), while a small and ephemeral Late Oligocene Warming was
366 present in the latest part of the Oligocene, resulting in reducing the Antarctic ice
367 sheets to a minimum and forming a brief period of glaciation at that time (Zachos et
368 al., 2001). During the Middle Miocene, a quick rise in temperature was shown, which
369 was followed by a small glaciation (Fig. 6; Zachos et al., 2001; Roth-Nebelsick et al.,
370 2004; Beerling and Royer, 2011). Subsequently, the CO_2 concentration decreased
371 gradually and reached 280 ppmv until the period of the industrial revolution (Fig. 6).
372 Since then, however, the CO_2 concentration rebounded to present day level.

373 In conclusion, although various results were made by different pCO_2 reconstruction

374 proxies at the same time, their entire decreasing tendency of pCO₂ level are
375 remarkably consistent with each other since the Eocene (Fig. 6). Fig. 6 shows that
376 during the Eocene the temperature was higher than at present. The reconstructed pCO₂
377 of 351.9 ± 6.6 ppmv based on the regression approach is shows a remarkably low
378 pCO₂ level during the early late Eocene. The result based on the stomatal ratio
379 method of 537.5 ± 56.5 ppmv is closely consistent with the pCO₂ changes over the
380 geological ages (Fig. 6).

381

382

383

384 **6 Conclusion**

385

386 In this study, we reconstructed the late Eocene pCO₂ based on the fossil leaves of
387 *Nageia maomingensis* Jin et Liu from the late Eocene of Maoming Basin, Guangdong
388 Province, China. *Nageia* is a special element in conifers by its broad multi-veined leaf
389 that lacks mid-vein. The stomatal data analysis suggests that only stomatal densities
390 (SD) from both sides of *Nageia motleyi* leaves have significant negative correlations
391 with the atmospheric CO₂ concentration. The SD from the adaxial side gives the best
392 correlation to the CO₂. Based on SDs, the pCO₂ concentration is reconstructed using
393 both the regression approach and the stomatal ratio method. The pCO₂ result based on
394 the regression approach is 351.9 ± 6.6 ppmv, showing a relatively lower CO₂ level.
395 The reconstructed result based on the stomatal ratio method is 537.5 ± 56.5 ppmv

396 consistent with the variation trends based on the other proxies. Here, we explored the
397 potential of *N. maomingensis* in pCO₂ reconstruction and obtained different results
398 according to different methods, providing a new insight for the reconstruction of
399 paleoclimate and paleoenvironment in conifers.

400

401 *Acknowledgements.* This study was supported by the National Natural Science
402 Foundation of China (Grant No. 41210001, 41572011), the Fundamental Research
403 Funds for the Central Universities (Grant No.12lgjc04), and the Key Project of Sun
404 Yat-sen University for inviting foreign teachers. We greatly thank the Herbarium of
405 the V.L. Komarov Botanical Institute of the Russian Academy of Sciences (LE) for
406 the permission to examine and collect extant *Nageia* specimens. We also express
407 sincere gratitude to Prof. Sun Tongxing (Yancheng Teachers University), Dr. David
408 Boufford (Harvard University) and Dr. Richard Chung Cheng Kong (Forest Research
409 Institute Malaysia) for providing extant *N. motleyi* leaves from the herbarium of the
410 Royal Botanic Garden at Edinburgh (E), the Harvard University Herbaria (A/GH) and
411 the herbarium of Forest Research Institute Malaysia (KEP). We sincerely appreciate
412 the guidance of Chengqian Wang (Harbin Institute of Technology) on preparing Figs.
413 3–6. We also offer sincere gratitude to Prof. Steven R. Manchester and Mr. Terry Lott
414 (Florida Museum of Natural History, University of Florida) for suggestions and
415 modification.

416 **References**

- 417 Bai, Y. J., Chen, L. Q., Rahnotra, S. P., Wang, Q., Wang, Y. F., Li, C. S.:
418 Reconstructing atmospheric CO₂ during the Plio–Pleistocene transition by fossil
419 *Typha*. *Global Change Biology*, 21, 874–881, doi:10.1111/gcb.12670, 2015.
- 420 Beerling, D. J.: Stomatal density and index: theory and application, in: Jones, T. P.,
421 and Rowe, N. P., (Eds.), *Fossil Plants and Spores: Modern Techniques*,
422 Geological Society, London, 251–256, 1999.
- 423 Beerling, D. J., and Kelly, C. K.: Stomatal density responses of temperate woodland
424 plants over the past seven decades of CO₂ increase: A comparison of salisbury
425 (1927) with contemporary data, *American Journal of Botany*, 84, 1572–1583,
426 1997.
- 427 Beerling, D. J., and Royer, D. L.: Reading a CO₂ signal from fossil stomata, *New*
428 *Phytologist*, 153, 387–397, doi:10.1046/j.0028-646X.2001.00335.x, 2002.
- 429 Beerling, D. J., and Royer, D. L.: Convergent Cenozoic CO₂ history, *Natural*
430 *Geoscience*, 4, 418–420, doi:10.1038/ngeo1186, 2011.
- 431 Beerling, D. J., Chaloner, W. G., Huntley, B., Pearson, J. A., Tooley, M. J., and
432 Woodward, F. I.: Variations in the stomatal density of *Salix herbacea* L. under
433 the changing atmospheric CO₂ concentrations of late- and post-glacial time,
434 *Philosophical Transactions of the Royal Society of London*, ser. B. 336, 215–224,
435 doi:10.1098/rstb.1992.0057, 1992.
- 436 Beerling, D. J., Fox, A., and Anderson, C. W.: Quantitative uncertainty analyses of
437 ancient atmospheric CO₂ estimates from fossil leaves, *American Journal of*

438 Science, 309, 775–787, doi:10.2475/09.2009.01, 2009.

439 Beerling, D. J., Lomax, B. H., Royer, D. L., Upchurch Jr., G. R., and Kump, L. R.: An
440 atmospheric $p\text{CO}_2$ reconstruction across the Cretaceous-Tertiary boundary from
441 leaf megafossils, Proceedings of the National Academy of Sciences of the United
442 States of America, 99, 7836–7840, doi:10.1073/pnas.122573099, 2002.

443 Berner, R. A.: GEOCARB II: A revised model of atmospheric CO_2 over Phanerozoic
444 time, American Journal of Science, 294, 56–91, doi:10.2475/ajs.294.1.56, 1994.

445 Berner, R. A., and Kothavalá Z.: GEOCARB III: A revised model of Atmospheric
446 CO_2 over Phanerozoic time, American Journal of Science, 301, 182–204,
447 doi:10.2475/ajs.301.2.182, 2001.

448 Bijl, P. K., Houben, A. J. P., Schouten, S., Bohaty, S. M., Sluijs, A., Reichart, G.,
449 Sinninghe Damsté J. S., and Brinkhuis, H.: Transient Middle Eocene
450 atmospheric CO_2 and temperature variations, Science, 330, 819–821,
451 doi:10.1126/science.1193654, 2010.

452 Brown, L. R.: Atmospheric carbon dioxide concentration, 1000-2009 (Supporting
453 data), in: Brown, L. R., (Ed.), World on the Edge: How to Prevent Environmental
454 and Economic Collapse. Chapter 4 Data: Rising Temperatures, Melting Ice, and
455 Food Security, Earth policy institute, Norton, W.W. & Company, New York,
456 London (http://www.earth-policy.org/books/wote/wote_data), 2010.

457 Cerling, T. E.: Carbon dioxide in the atmosphere: evidence from Cenozoic and
458 Mesozoic palaeosols, American Journal of Science, 291, 377–400,
459 doi:10.2475/ajs.291.4.377, 1991.

460 Cerling, T. E.: Use of carbon isotopes in paleosols as an indicator of the P(CO₂) of the
461 paleoatmosphere, *Global Biogeochemical Cycles*, 6, 307–314,
462 doi:10.1029/92GB01102, 1992.

463 Chaloner, W. G., and McElwain, J. C.: The fossil plant record and global climate
464 change, *Review of Palaeobotany and Palynology*, 95, 73–82,
465 doi:10.1016/S0034-6667(96)00028-0, 1997.

466 Cheng, W. C., Fu, L. K., and Chao, C. S.: *Podocarpus* (Podocarpaceae), in: Cheng,
467 Wanch ün, and Fu, Likuo, (Eds.), *Flora of China*, Science Press, Beijing, 7,
468 398–422, 1978 (in Chinese).

469 Doria, G., Royer, D. L., Wolfe, A. P., Fox, A., Westgate, J. A., and Beerling, D. J.:
470 Declining atmospheric CO₂ during the Late Middle Eocene climate transition,
471 *American Journal of Science*, 311, 63–75, doi:10.2475/01.2011.03, 2011.

472 Ekart, D. D., Cerling, T. E., Montanez, I. P., and Tabor, N. J.: A 400 million year
473 carbon isotope record of pedogenic carbonate: implications for paleoatmospheric
474 carbon dioxide, *American Journal of Science*, 299, 805–827,
475 doi:10.2475/ajs.299.10.805, 1999.

476 Fletcher, B. J., Brentnall, S. J., Anderson, C. W., Berner, R. A., and Beerling, D. J.:
477 Atmospheric carbon dioxide linked with Mesozoic and Early Cenozoic climate
478 change, *Nature Geoscience*, 1, 43–48, doi:10.1038/ngeo.2007.29, 2008.

479 Freeman, K. H., and Hayes, J. M.: Fractionation of carbon isotopes by phytoplankton
480 and estimates of ancient CO₂ levels, *Global Biogeochemical Cycles*, 6, 185–198,
481 doi:10.1029/92GB00190, 1992.

482 Fu, D. Z.: Nageiaceae – a new gymnosperm family, *Acta Phytotaxonomica Sinica*, 30,
483 515–528, 1992 (in Chinese with English summary).

484 Fu L. K., Li Y., and Mill, R. R.: Podocarpaceae, in: Wu Z. Y., and Raven, P. H., (Eds.),
485 *Flora of China*, Science Press, Beijing, 4, 78–84, 1999.

486 Gale, J.: Availability of carbon dioxide for photosynthesis at high altitudes: theoretical
487 considerations, *Ecology*, 53, 494–497, doi:10.2307/1934239, 1972.

488 Greenwood, D. G., Scarr, M. J., and Christophel, D. C.: Leaf stomatal frequency in the
489 Australian tropical rain forest tree *Neolitseadealbata* (Lauraceae) as a proxy
490 measure of atmospheric $p\text{CO}_2$, *Palaeogeography, Palaeoclimatology,*
491 *Palaeoecology*, 196, 375–393, doi:10.1016/S0031-0182(03)00465-6, 2003.

492 Grein, M., Oehm, C., Konrad, W., Utescher, T., Kunzmann, L., and Roth-Nebelsick,
493 A.: Atmospheric CO_2 from the late Oligocene to early Miocene based on
494 photosynthesis data and fossil leaf characteristics, *Palaeogeography,*
495 *Palaeoclimatology, Palaeoecology*, 374, 41–51,
496 doi:10.1016/j.palaeo.2012.12.025, 2013.

497 Henderiks, J., and Pagani, M.: Coccolithophore cell size and the Paleogene decline in
498 atmospheric CO_2 , *Earth and Planetary Science Letters* 269, 575–583,
499 doi:10.1016/j.epsl.2008.03.016, 2008.

500 Hill, R. S., and Pole, M. S.: Leaf and shoot morphology of extant *Afrocarpus*, *Nageia*
501 and *Retrophyllum* (Podocarpaceae) species, and species with similar leaf
502 arrangement, from Tertiary sediments in Australasia, *Australian Systematic*
503 *Botany*, 5, 337–358, doi:10.1071/SB9920337, 1992.

504 Hu, J. J., Xing, Y. W., Turkington, R., Jacques, F. M. B. Su, T., Huang, Y. J. and Zhou
505 Z. K.: A new positive relationship between pCO₂ and stomatal frequency in
506 *Quercus guyavifolia* (Fagaceae): a potential proxy for palaeo-CO₂ levels, *Annals*
507 *of Botany*, 1–12, doi:10.1093/aob/mcv007, 2015.

508 Huang, C., Retallack, G. J., Wang, C., and Huang, Q.: Paleoatmospheric pCO₂
509 fluctuations across the Cretaceous-Tertiary boundary recorded from paleosol
510 carbonates in NE China, *Palaeogeography, Palaeoclimatology, Palaeoecology*,
511 385, 95–105, doi.org/10.1016/j.palaeo.2013.01.005, 2013.

512 Jacques, F. M. B., Shi, G. L., Li, H. M., and Wang, W. M.: An Early-Middle Eocene
513 Antarctic summer monsoon: Evidence of ‘fossil climates’, *Gondwana Research*,
514 25, 1422–1428, doi:10.1016/j.gr.2012.08.007, 2014.

515 Jin, J. H., Qiu, J., Zhu, Y. A., and Kodrul, T. M.: First fossil record of the genus
516 *Nageia* (Podocarpaceae) in South China and its phytogeographic implications,
517 *Plant Systematics and Evolution*, 285, 159–163, doi:10.1007/s00606-010-0267-4,
518 2010.

519 Jones, H. G.: *Plants and microclimate*, Cambridge UK Cambridge University Press,
520 1–428, 1992.

521 Kato, Y., Fujinaga, K., and Suzuki, K.: Marine Os isotopic fluctuations in the Early
522 Eocene greenhouse interval as recorded by metalliferous umbers from a Tertiary
523 ophiolite in Japan, *Gondwana Research*, 20, 594–607,
524 doi:10.1016/j.gr.2010.12.007, 2011.

525 Keating-Bitonti, C. R., Ivany, L. C., Affek, H. P., Douglas, P., and Samson, S. D.:

526 Warm, not super-hot, temperatures in the early Eocene subtropics, *Geology* 39,
527 771–774, doi: 10.1130/G32054.1, 2011.

528 Kimura, T., Ohana, T., and Mimoto, K.: Discovery of a podocarpaceous plant from
529 the Lower Cretaceous of Kochi Prefecture, in the outer zone of southwest Japan,
530 *Proceedings of the Japan Academy, ser. B*, 64, 213–216, doi:10.2183/pjab.64.213,
531 1988.

532 Koch, P. L., Zachos, J. C., and Gingerich, P. D.: Correlation between isotope records
533 in marine and continental carbon reservoirs near the Palaeocene/Eocene
534 boundary, *Nature*, 358, 319–322, doi:10.1038/358319a0, 1992.

535 Kouwenberg, L. L. R., McElwain J. C., Kürschner, W. M., Wagner, F., Beerling, S. J.,
536 Mayle, F. E., and Visscher, H.: stomatal frequency adjustment of four conifer
537 species to historical changes in atmospheric CO₂, *American Journal of Botany*,
538 90, 610–619, 2003.

539 Körner, Ch., and Cochrane, P. M.: Stomatal responses and water relations of
540 *Eucalyptus pauciflora* in summer along an elevational gradient, *Oecologia*, 66,
541 443–455, doi:10.1007/BF00378313, 1985.

542 Krassilov, V. A.: New coniferales from Lower Cretaceous of Primorye, *Botanical*
543 *Journal*, 50, 1450–1455 (in Russia), 1965.

544 Kürschner, W. M., van der Burgh, J., Visscher, H., and Dilcher, D. L.: Oak leaves as
545 biosensors of Late Neogene and Early Pleistocene paleoatmospheric CO₂
546 concentrations, *Marine Micropaleontology*, 27, 299–312,
547 doi:10.1016/0377-8398(95)00067-4, 1996.

548 Kürschner, W. M., Wagner, F., Dilcher, D. L., and Visscher, H.: Using fossil leaves for
549 the reconstruction of Cenozoic paleoatmospheric CO₂ concentrations, in:
550 Gerhard, L. C., Harrison, W. E., Hanson, B. M., (Eds.), Geological Perspectives
551 of Global Climate Change, APPG Studies in Geology, 47, Tulsa, 169–189, 2001.

552 Kürschner, W. M., Kvaček, Z., and Dilcher, D. L.: The impact of Miocene
553 atmospheric carbon dioxide fluctuations on climate and the evolution of
554 terrestrial ecosystems, Proceedings of the National Academy of Sciences of the
555 United States of America, 105, 449–453, doi:10.1073/pnas.0708588105, 2008.

556 Liu, X. Y., Gao, Q., and Jin, J. H.: Late Eocene leaves of *Nageia* Gaertner (section
557 *Dammaroideae* Mill) from Maoming Basin, South China and their implications
558 on phytogeography, Journal of Systematics and Evolution, 53, 297–307,
559 doi:10.1111/jse.12133, 2015.

560 Lowenstein, T. K., and Demicco, R. V.: Elevated Eocene atmospheric CO₂ and its
561 subsequent decline, Science, 313, 1928, doi:10.1126/science.1129555, 2006.

562 McElwain, J. C.: Do fossil plants signal palaeoatmospheric carbon dioxide
563 concentration in the geological past, Philosophical Transactions of the Royal
564 Society, Lond B, 353, 83–96, doi:10.1098/rstb.1998.0193, 1998.

565 McElwain, J. C., and Chaloner, W. G.: Stomatal density and index of fossil plants
566 track atmospheric carbon dioxide in the Palaeozoic, Annals of Botany, 76,
567 389–395, doi:10.1006/anbo.1995.1112, 1995.

568 McElwain, J. C., and Chaloner, W. G.: The fossil cuticle as a skeletal record of
569 environmental changes, Palaios, 11, 376–388, doi: 10.2307/3515247, 1996.

570 Mill, R. R.: A new combination in *Nageia* (Podocarpaceae): *Novon*, 9, 77–78, 1999.

571 Mill, R. R.: A new sectional combination in *Nageia* Gaertn (Podocarpaceae),
572 *Edinburgh Journal of Botany*, 58, 499–501, doi:10.1017/S0960428601000804,
573 2001.

574 Maxbauer, D. P., Royer, D. L., and LePage, B. A.: High Arctic forests during the
575 middle Eocene supported by moderate levels of atmospheric CO₂, *Geology*, 42,
576 1027–1030, doi:10.1130/G36014.1, 2014.

577 Moran, K., Backman, J., Brinkhuis, H., Clemens, S. C., Cronin, T., Dickens, G. R.,
578 Eynaud, F., Gattacceca, J., Jakobsson, M., Jordan, R. W., Kaminski, M., King, J.,
579 Koc, N., Krylov, A., Martinez, N., Matthiessen, J., McInroy, D., Moore, T.C.,
580 Onodera, J., O'Regan, M., Päike, H., Rea, B., Rio, D., Sakamoto, T., Smith, D.
581 C., Stein, R., St John, K., Suto, I., Suzuki, N., Takahashi, K., Watanabe, M.,
582 Yamamoto, M., Farrell, J., Frank, M., Kubik, P., Jokat, W., and Kristoffersen, Y.:
583 The Cenozoic palaeoenvironment of the Arctic Ocean, *Nature*, 441, 601–605,
584 doi:10.1038/nature04800, 2006.

585 Nordt, L., Atchley, S., and Dworkin, S. I.: Paleosol barometer indicates extreme
586 fluctuations in atmospheric CO₂ across the Cretaceous-Tertiary boundary,
587 *Geology*, 30, 703–706, doi:10.1130/0091-7613(2002)030<0703:PBIEFI>
588 2.0.CO;2, 2002.

589 Pagani, M., Arthur, M. A., and Freeman, K. H.: Miocene evolution of atmospheric
590 carbon dioxide, *Paleoceanography*, 14, doi:10.1029/1999PA900006, 273–292,
591 1999.

592 Pagani, M., Zachos, J. C., Freeman, K. H., Tipple, B., and Bohaty, S.: Marked decline
593 in atmospheric carbon dioxide concentrations during the Paleocene, *Science*, 309,
594 600–603, doi:10.1126/science.1110063, 2005.

595 Pearson, P. N., Foster, G. L., and Wade, B. S.: Atmospheric carbon dioxide through the
596 Eocene-Oligocene climate transition, *Nature*, 461, 1110–1113,
597 doi:10.1038/nature08447, 2009.

598 Petit, J. R., Jouzel, J., Raynaud, D., Barkov, N. I., Barnola, J.-M., Basile, I., Bender,
599 M., Chappellaz, J., Davis, M., Delaygue, G., Delmotte, M., Kotlyakov, V. M.,
600 Legrand, M., Lipenkov, V. Y., Lorius, C., PÉpin, L., Ritz, C., Saltzman, E., and
601 Stievenard, M.: Climate and atmospheric history of the past 420,000 years from
602 the Vostokicecore, Antarctica, *Nature*, 399, 429–436, doi:10.1038/20859, 1999.

603 Pieter, T., and Keeling, R.: Recent monthly average Mauna Loa CO₂, NOAA/ESRL,
604 www.esrl.noaa.gov/gmd/ccgg/trends/ (accessed March 2015), 2015.

605 Poole, I., and Kürschner, W. M.: Stomatal density and index: the practice, in: Jones,
606 T.P., and Rowe, N.P., (Eds.), *Fossil Plants and Spores: Modern Techniques*,
607 Geological Society, London, 257–260, 1999.

608 Retallack, G. J.: A 300-million-year record of atmospheric carbon dioxide from fossil
609 plant cuticles, *Nature*, 411, 287–290, doi:10.1038/35077041, 2001.

610 Retallack, G. J.: Greenhouse crises of the past 300 million years, *Geological Society*
611 *of America Bulletin*, 121, 1441–1455, doi:10.1130/B26341.1, 2009a.

612 Retallack, G. J.: Refining a pedogenic-carbonate CO₂ paleobarometer to quantify a
613 Middle Miocene greenhouse spike, *Palaeogeography, Palaeoclimatology*,

614 Palaeoecology, 281, 57–65, doi:10.1016/j.palaeo.2009.07.011, 2009b.

615 Roth-Nebelsick, A., Utescher, T., Mosbrugger, V., Diester-Haass, L., and Walther, H.:
616 Changes in atmospheric CO₂ concentrations and climate from the Late Eocene to
617 Early Miocene: palaeobotanical reconstruction based on fossil floras from
618 Saxony, Germany, Palaeogeography, Palaeoclimatology, Palaeoecology, 205,
619 43–67, doi:10.1016/j.palaeo.2003.11.014, 2004.

620 Roth-Nebelsick, A., Grein, M., Utescher, T., and Konrad, W.: Stomatal pore length
621 change in leaves of *Eotrigonobalanus furcinervis* (Fagaceae) from the Late
622 Eocene to the Latest Oligocene and its impact on gas exchange and CO₂
623 reconstruction, Review of Palaeobotany and Palynology, 174, 106–112,
624 doi:10.1016/j.revpalbo.2012.01.001, 2012.

625 Roth-Nebelsick, A., Oehm, C., Grein, M., Utescher, T., Kunzmann, L., Friedrich, J.-P.,
626 and Konrad, W.: Stomatal density and index data of *Platanus neptuni* leaf fossils
627 and their evaluation as a CO₂ proxy for the Oligocene, Review of Palaeobotany
628 and Palynology, 206, 1–9, doi:10.1016/j.revpalbo.2014.03.001, 2014.

629 Royer, D. L.: Stomatal density and stomatal index as indicators of paleoatmospheric
630 CO₂ concentration, Review of Palaeobotany and Palynology, 114, 1–28,
631 doi:10.1016/S0034-6667(00)00074-9, 2001.

632 Royer, D. L.: Estimating Latest Cretaceous and Tertiary atmospheric CO₂ from
633 stomatal indices, in: Wing, S. L., Gingerich, P. D., Schmitz, B., and Thomas, E.,
634 (Eds.), Causes and Consequences of Globally Warm Climates in the Early
635 Paleocene, Geological Society of America Special Paper, 79–93, 2003.

636 Royer, D. L.: CO₂-forced climate thresholds during the Phanerozoic, *Geochimica et*
637 *Cosmochimica Acta*, 70, 5665–5675, doi:10.1016/j.gca.2005.11.031, 2006.

638 Royer, D. L., Wing, S. L., Beerling, D. J., Jolley, D. W., Koch, P. L., Hickey, L. J., and
639 Berner, R. A.: Paleobotanical evidence for near present-day levels of atmospheric
640 CO₂ during part of the Tertiary, *Science*, 292, 2310–2313,
641 doi:10.1126/science.292.5525.2310, 2001.

642 Rundgren, M., and Beerling, D. J.: A Holocene CO₂ record from the stomatal index of
643 subfossil *Salix herbacea* L. leaves from northern Sweden, *The Holocene*, 9,
644 509–513, doi:10.1191/095968399677717287, 1999.

645 Seki, O, Foster, G. L., Schmidt, D. N., Mackensen, A., Kawamura, K., and Pancost, R.
646 D.: Alkenone and boron-based Pliocene *p*CO₂ records, *Earth and Planetary*
647 *Science Letters*, 292, 201–211, doi:10.1016/j.epsl.2010.01.037, 2010.

648 Sinha, A., and Stott, L. D.: New atmospheric *p*CO₂ estimates from paleosols during
649 the late Paleocene/early Eocene global warming interval, *Global and Planetary*
650 *Change*, 9, 297–307, doi:10.1016/0921-8181(94)00010-7, 1994,

651 Smith, R. Y., Greenwood, D. R., and Basinger, J.F.: Estimating paleoatmospheric
652 *p*CO₂ during the Early Eocene Climatic Optimum from stomatal frequency of
653 *Ginkgo*, Okanagan Highlands, British Columbia, Canada, *Palaeogeography,*
654 *Palaeoclimatology, Palaeoecology*, 293, 120–131,
655 doi:10.1016/j.palaeo.2010.05.006, 2010.

656 Spicer, A. R., Herman, A. B., Liao, W. B., Spicer, T. E. V., Kodrul, T. M., Yang, J., and
657 Jin, J. H.: Cool tropics in the middle Eocene: Evidence from the Changchang

658 Flora, Hainan Island, China, *Palaeogeography, Palaeoclimatology, Palaeoecology*,
659 412, 1–16, doi:10.1016/j.palaeo.2014.07.011, 2014.

660 Stott, L. D.: Higher temperatures and lower oceanic $p\text{CO}_2$: A climate enigma at the
661 end of the Paleocene Epoch, *Paleoceanography*, 7, 395–404,
662 doi:10.1029/92PA01183, 1992.

663 Stults, D. Z., Wagner-Cremer, F., and Axsmith, B. J.: Atmospheric paleo- CO_2
664 estimates based on *Taxodium distichum* (Cupressaceae) fossils from the Miocene
665 and Pliocene of Eastern North America, *Palaeogeography Palaeoclimatology*
666 *Palaeoecology*, 309, 327–332, doi:10.1016/j.palaeo.2011.06.017, 2011.

667 Sun, B. N., Ding, S. T., Wu, J. Y., Dong, C., Xie, S. P., and Lin, Z. C.: Carbon isotope
668 and stomatal data of Late Pliocene Betulaceae leaves from SW China:
669 Implications for palaeoatmospheric CO_2 -levels, *Turkish Journal of Earth*
670 *Sciences*, 21, 237–250, doi:10.3906/yer-1003-42, 2012.

671 Sun, T. X.: Cuticle micromorphology of *Nageia*, *Journal of Wuhan Botanical*
672 *Research*, 26, 554–560, doi:10.3969/j.issn.2095-0837.2008.06.002, 2008 (in
673 Chinese with English abstract).

674 Tripathi, A. K., Roberts, C. D., and Eagle, R. A.: Coupling of CO_2 and ice sheet
675 stability over major climate transitions of the last 20 million years, *Science*, 326,
676 1394–1397, doi:10.1126/science.1178296, 2009.

677 Van der Burgh, J., Visscher, H., Dilcher, D. L., and Kürschner, W. M.:
678 Paleoatmospheric signatures in Neogene fossil leaves, *Science*, 260, 1788–1790,
679 doi:10.1126/science.260.5115.1788, 1993.

680 Wang, J. D., Li, H. M., and Zhu Z. Y.: Magnetostratigraphy of Tertiary rocks from
681 Maoming Basin, Guangdong province, China, Chinese Journal of Geochemistry,
682 13, 165–175, doi:10.1007/BF02838516, 1994.

683 Wing, S. L., Harrington, G. J., Smith, F. A., Bloch, J. I., Boyer, D. M., and Freeman, K.
684 H.: Transient floral change and rapid global warming at the Paleocene-Eocene
685 boundary, Science, 310, 993–996, doi:10.1126/science.1116913, 2005.

686 Woodward, F. I.: Ecophysiological studies on the shrub *Vaccinium myrtillus* L. taken
687 from a wide altitudinal range, Oecologia, 70, 580–586, doi:10.1007/BF00379908,
688 1986.

689 Woodward, F. I.: Stomatal numbers are sensitive to increases in CO₂ concentration
690 from pre-industrial levels, Nature, 327, 617–618, doi:10.1038/327617a0, 1987.

691 Woodward, F. I., and Bazzaz, F. A.: The responses of stomatal density to CO₂ partial
692 pressure, Journal of Experimental Botany, 39, 1771–1781,
693 doi:10.1093/jxb/39.12.1771, 1988.

694 Yang, J. J., Qi, G. F., and Xu, R. H.: Studies on fossil woods excavated from the Dabie
695 mountains, Scientia Silvae Sinicae, 26, 379–386, 1990 (in Chinese with English
696 abstract).

697 Ye, M. N.: On the preparation methods of fossil cuticle. Palaeontological Society of
698 China (Ed.), Selected papers of the 12th Annual conference of the
699 Palaeontological Society of China, Science Press, Beijing, 170–179, 1981 (in
700 Chinese).

701 Zachos, J., Pagani, M., Sloan, L., Thomas, E., and Billups, K.: Trends, rhythms,

702 aberrations in global climate 65 Ma to present, *Science*, 292, 686–693,
703 doi:10.1126/science.1059412, 2001.

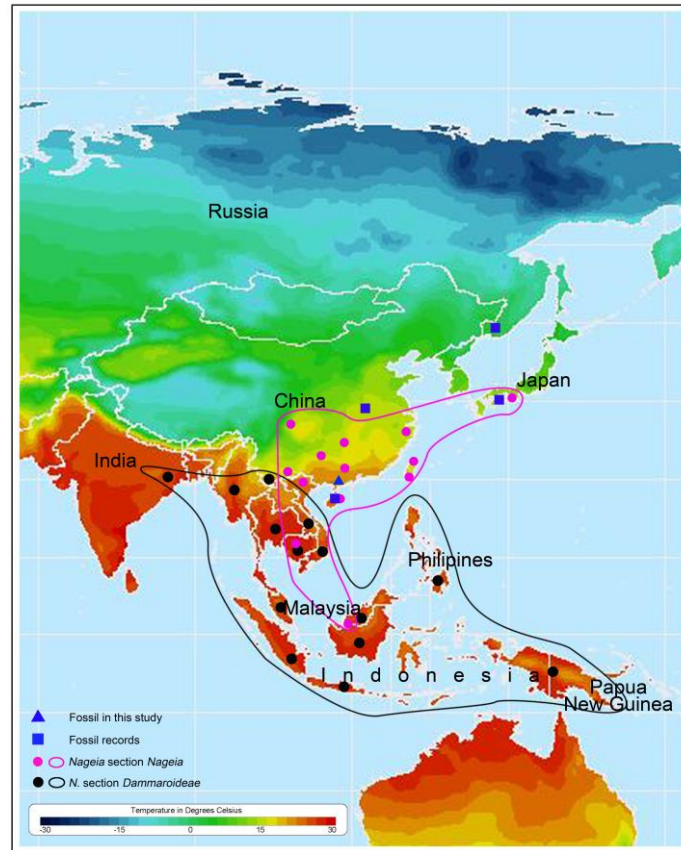
704 Zachos, J., Dickens, G. R. and Zeebe, R. E.: An early Cenozoic perspective on
705 greenhouse warming and carbon-cycle dynamics, *Nature*, 451, 279–283,
706 doi:10.1038/nature06588, 2008.

707

708 Figure 1. Map showing the distribution of extant and fossil *Nageia* and their mean annual

709 temperature (Modified after the map from

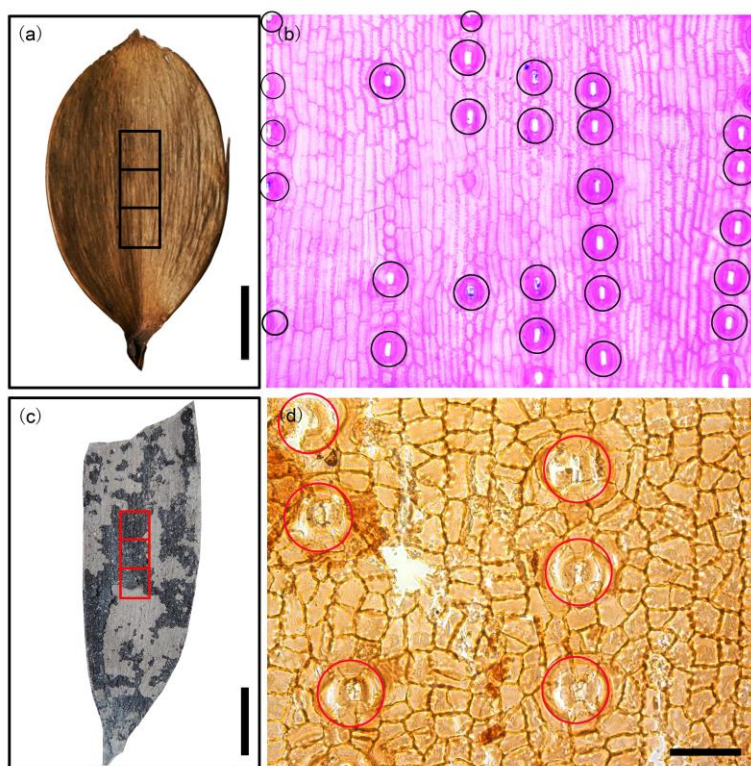
710 <http://www.sage.wisc.edu/atlas/maps.php?datasetid=35&includerelatedlinks=1&dataset=35>).



711

712

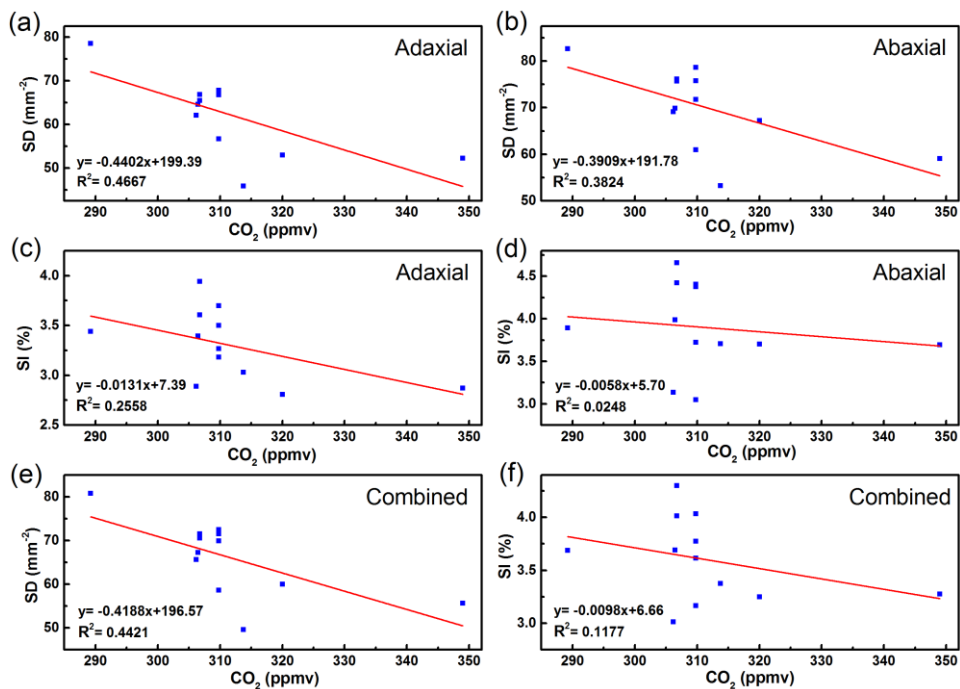
713 Figure 2. Sampling areas and counting rules are shown. (a) *Nageia motleyi* (Parl.) De Laub.leaf.
714 Black squares in the middle of the leaf show the sampling areas for preparing the cuticles. (b) The
715 abaxial side of the cuticle from *N. motleyi* leaf. Black circles show the counted stomatal
716 complexes. (c) *N. maomingensis* Jin et Liu. Red squares in the middle of the leaf indicate the
717 sampling areas. (d) The abaxial side of the fossil cuticle. Red circles show the counted stomatal
718 complexes. Scale bars: (a) and (c) = 1 cm; (b) and (d) = 50 μ m.



719

720

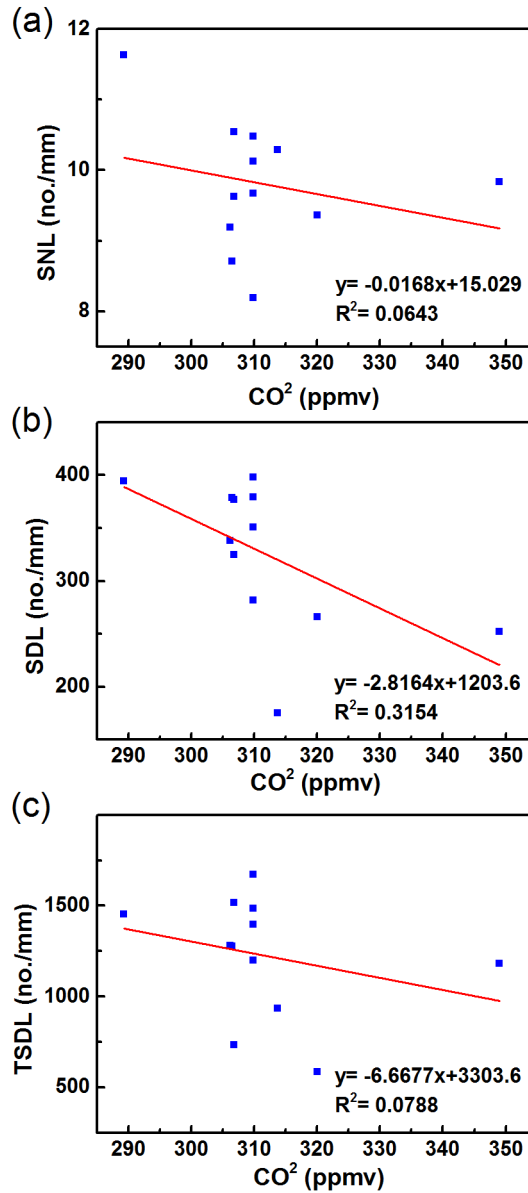
721 Figure 3. Correlation between SD and SI versus CO₂ concentration for modern *Nageia motleyi*. (a)
 722 Trends of SD with CO₂ concentration for the adaxial surface. (b) Trends of SD with CO₂
 723 concentration for the abaxial surface. (c) Trends of SI with CO₂ concentration for the adaxial
 724 surface. (d) Trends of SI with CO₂ concentration for the abaxial surface. (e) Trends of SD with
 725 CO₂ concentration for the combined data of both leaf surfaces. (f) Trends of SI with CO₂
 726 concentration for the combined data of both leaf surfaces.



727

728

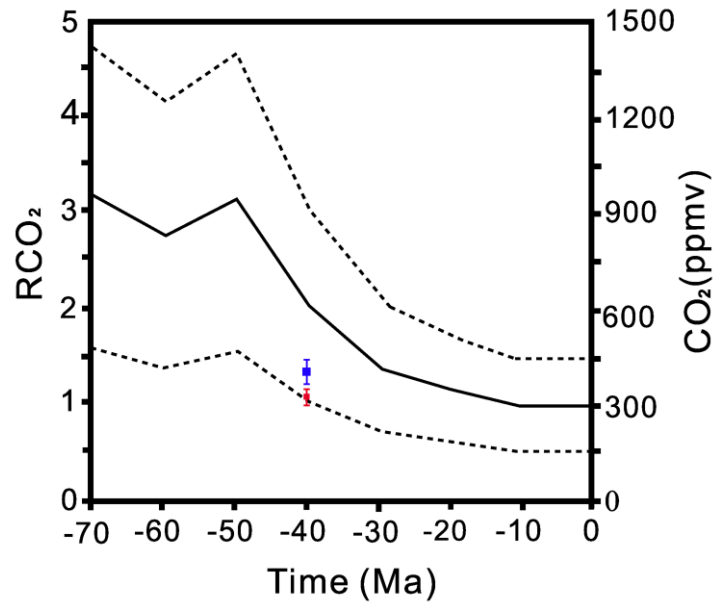
729 Figure 4. Correlation between SNL, SDL and TSDL versus CO₂ concentration for modern *Nageia*
730 *motleyi*. (a) Trends of SNL with CO₂ concentration for the adaxial surface. (b) Trends of SDL with
731 CO₂ concentration for the adaxial surface. (c) Trends of TSDL with CO₂ concentration for the
732 adaxial surface.



733

734

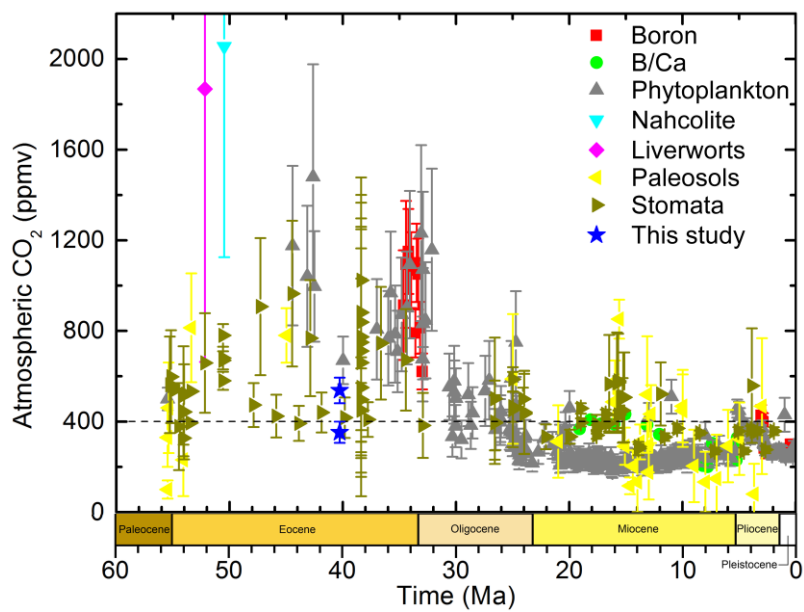
735 Figure 5. The pCO₂ reconstruction results and extant CO₂ concentrations are projected onto the
736 long-term carbon cycle model (GEOCARB III; Berner and Kothavala 2001). The pCO₂ results
737 based on the regression approach and stomatal ratio method are represented by red and blue
738 squares, respectively.



739

740

741 Figure 6. Atmospheric CO₂ estimates from proxies over the past 60 million years. The horizontal
 742 dashed line indicates monthly atmospheric CO₂ concentration for March 2015 at Mauna Loa,
 743 Hawaii (401.5 ppmv) (Pieter and Keeling, 2015). The vertical lines show the error bars. The data
 744 are from the supporting data of Beerling and Royer (2011) and references in Table 9. The lower
 745 blue star shows the reconstructed result based on the regression approach. The higher one presents
 746 the result of stomatal ratio method.



747

748 Table 1. Modern *Nageia motleyi* (Parl.) De Laub samples and atmospheric CO₂ values of their collection dates from ice core data (Brown, 2010).

749

| Herbarium | Collection number | Collecting locality | Collectors | Number of leaf samples | Collection date | CO ₂ (ppmv) |
|-----------|-------------------|---------------------------------------------------------------------------------------------|-----------------------------------|------------------------|-----------------|------------------------|
| LE | No. 2649 | Malaysia | Beccari, O. | 1 | 1868 | 289.23 |
| A/GH | No. bb. 17229 | 150 m, Riau on Ond. Karimon, Archipel. Ind. | Neth. Ind. For. Service | 2 | 1932 | 306.19 |
| A/GH | No. bb. 18328 | 5 m, Z. O. afd. v. Borneo Tidoengsche Landen, Archipel. Ind. | Neth. Ind. For. Service | 2 | 1934 | 306.46 |
| A/GH | No. bb. 21151 | 500 m, Z. O. afd. Borneo, Poeroek Tjahoe Tahoedjan, Archipel. Ind. | Neth. Ind. For. Service | 2 | 1936 | 306.76 |
| KEP | No. 30887 | Kata Tinggi, Johor, Malaysia | Corner, E.J.H. | 1 | 1936 | 306.76 |
| KEP | No. 57329 | Batang Padang, Perak, Malaysia | Unkonwn | 2 | 1947 | 309.82 |
| KEP | No. 57330 | Batang Padang, Perak, Malaysia | Unkonwn | 2 | 1947 | 309.82 |
| KEP | No. 55897 | Batang Padang, Perak, Malaysia | Unkonwn | 2 | 1947 | 309.82 |
| KEP | No. 61064 | Batang Padang, Perak, Malaysia | Syed Woh | 2 | 1947 | 309.82 |
| E | No. bb. 40798 | 51 m, Kuala Trengganu-Besut Road, Bukit Bintang Block, Gunong Tebu Forest reserve, Malaysia | Sinclair, J. and Kiah bin, Salleh | 2 | 1955 | 313.73 |
| KEP | No. 80548 | Gombak, Selangor, Malaysia | Rahim | 1 | 1965 | 320.04 |
| KEP | No. 33343 | Jelevu, Negeri Sembilan, Malaysia | Yap, S.K. | 2 | 1987 | 348.98 |

Note: A/GH—Harvard University Herbarium, Harvard University, 22 Divinity Avenue, Cambridge, Massachusetts 02138, USA (www.huh.harvard.edu).

E—The Herbarium of Royal Botanic Garden, Edinburgh EH3 5LR, Scotland, UK (www.rbge.org.uk).

LE—The Herbarium of the V.L. Komarov Botanical Institute of the Russian Academy of Sciences, Prof. Popov Street 2, Saint Petersburg 197376, Russia (www.binran.ru).

KEP—Kepong Herbarium, Forest Research Institute Malaysia, 52109 Kepong, Selangor, Malaysia (<http://www.frim.gov.my/>).

750 Table 2. Summary of stomatal parameters of the adaxial surface from modern *Nageia motleyi* (Parl.) De Laub.

| Collection number | Collection date | CO ₂ (ppmv) | SD (mm ⁻²) | | | | | SI (%) | | | | |
|-------------------|-----------------|------------------------|------------------------|----------|------|--------|-----|----------|----------|------|--------|-----|
| | | | <i>x</i> | σ | s.e. | t*s.e. | n | <i>x</i> | σ | s.e. | t*s.e. | n |
| No.2649 | 1868 | 289.23 | 78.60 | 15.44 | 1.41 | 2.76 | 120 | 3.44 | 0.66 | 0.06 | 0.12 | 120 |
| No.bb.17229 | 1932 | 306.19 | 62.14 | 17.20 | 1.78 | 3.50 | 93 | 2.89 | 0.68 | 0.07 | 0.14 | 93 |
| No.bb.18328 | 1934 | 306.46 | 64.57 | 15.05 | 1.58 | 3.11 | 90 | 3.39 | 1.01 | 0.11 | 0.21 | 90 |
| No.bb.21151 | 1936 | 306.76 | 65.45 | 11.14 | 1.17 | 2.30 | 90 | 3.94 | 0.74 | 0.08 | 0.15 | 90 |
| No.SFN30887 | 1936 | 306.76 | 66.90 | 16.10 | 1.27 | 2.49 | 161 | 3.61 | 0.92 | 0.07 | 0.14 | 161 |
| No.61064 | 1947 | 309.82 | 56.71 | 16.81 | 1.95 | 3.83 | 74 | 3.27 | 1.26 | 0.15 | 0.29 | 74 |
| No.57330 | 1947 | 309.82 | 67.37 | 15.97 | 2.04 | 4.01 | 61 | 3.70 | 0.82 | 0.10 | 0.20 | 61 |
| No.57329 | 1947 | 309.82 | 67.85 | 15.61 | 1.70 | 3.34 | 84 | 3.50 | 0.90 | 0.10 | 0.20 | 84 |
| No.55897 | 1947 | 309.82 | 66.74 | 14.10 | 1.78 | 3.48 | 63 | 3.18 | 0.66 | 0.08 | 0.16 | 63 |
| No.40798 | 1955 | 313.73 | 45.89 | 13.81 | 1.12 | 2.20 | 151 | 3.03 | 0.87 | 0.07 | 0.14 | 151 |
| No.KEP80548 | 1965 | 320.04 | 52.94 | 11.25 | 0.85 | 1.67 | 175 | 2.81 | 0.61 | 0.05 | 0.09 | 175 |
| No.FRI33343 | 1987 | 348.98 | 52.25 | 12.05 | 0.77 | 1.51 | 242 | 2.87 | 0.69 | 0.04 | 0.09 | 242 |
| Mean | — | — | 62.28 | 14.54 | 1.45 | 2.85 | 117 | 3.30 | 0.52 | 0.08 | 0.16 | 117 |

Note: *x*—mean; σ —standard deviation; s.e. —standard error of mean; n— numbers of photos counts (40 \times); t*s.e.— 95% confidence interval.

751 Table 3. Summary of stomatal parameters of the abaxial surface from modern *Nageia motleyi* (Parl.) De Laub.

| Collection number | Collection date | CO ₂ (ppmv) | SD (mm ⁻²) | | | | | SI (%) | | | | |
|-------------------|-----------------|------------------------|------------------------|----------|------|--------|-----|----------|----------|------|--------|-----|
| | | | <i>x</i> | σ | s.e. | t*s.e. | n | <i>x</i> | σ | s.e. | t*s.e. | n |
| No.2649 | 1868 | 289.23 | 82.71 | 12.23 | 1.02 | 2.00 | 144 | 3.89 | 0.58 | 0.05 | 0.09 | 144 |
| No.bb.17229 | 1932 | 306.19 | 69.16 | 14.23 | 1.48 | 2.90 | 93 | 3.13 | 0.58 | 0.06 | 0.12 | 93 |
| No.bb.18328 | 1934 | 306.46 | 69.92 | 14.38 | 1.52 | 2.97 | 90 | 3.99 | 1.08 | 0.11 | 0.22 | 90 |
| No.bb.21151 | 1936 | 306.76 | 75.68 | 15.74 | 1.66 | 3.25 | 90 | 4.66 | 0.88 | 0.09 | 0.18 | 90 |
| No.SFN30887 | 1936 | 306.76 | 76.18 | 12.51 | 0.99 | 1.93 | 161 | 4.42 | 0.89 | 0.07 | 0.14 | 161 |
| No.61064 | 1947 | 309.82 | 60.93 | 11.02 | 1.39 | 2.72 | 63 | 3.05 | 0.62 | 0.08 | 0.15 | 63 |
| No.57330 | 1947 | 309.82 | 75.82 | 14.14 | 1.82 | 3.58 | 60 | 4.38 | 0.84 | 0.11 | 0.21 | 60 |
| No.57329 | 1947 | 309.82 | 71.74 | 16.84 | 1.75 | 3.42 | 93 | 3.72 | 0.62 | 0.06 | 0.13 | 93 |
| No.55897 | 1947 | 309.82 | 78.63 | 13.41 | 1.75 | 3.42 | 59 | 4.41 | 1.00 | 0.13 | 0.26 | 59 |
| No.40798 | 1955 | 313.73 | 53.22 | 13.88 | 1.12 | 2.19 | 155 | 3.71 | 0.93 | 0.07 | 0.15 | 155 |
| No.KEP80548 | 1965 | 320.04 | 67.22 | 13.97 | 1.07 | 2.09 | 171 | 3.70 | 0.80 | 0.06 | 0.12 | 171 |
| No.FRI33343 | 1987 | 348.98 | 59.09 | 12.10 | 0.79 | 1.55 | 233 | 3.69 | 0.86 | 0.06 | 0.11 | 233 |
| Mean | — | — | 70.03 | 13.70 | 1.36 | 2.67 | 118 | 3.90 | 0.81 | 0.08 | 0.16 | 118 |

Note: *x*—mean; σ —standard deviation; s.e. —standard error of mean; n— numbers of photos counts (40×); t*s.e.— 95% confidence interval.

752

753 Table 4. Summary of stomatal parameters of the combined data of the adaxial and abaxial surfaces from modern *Nageia motleyi* (Parl.) De Laub.

| Collection number | Collection date | CO ₂ (ppmv) | SD (mm ⁻²) | | | | | SI (%) | | | | |
|-------------------|-----------------|------------------------|------------------------|----------|------|--------|-----|----------|----------|------|--------|-----|
| | | | <i>x</i> | σ | s.e. | t*s.e. | n | <i>x</i> | σ | s.e. | t*s.e. | n |
| No.2649 | 1868 | 289.23 | 80.84 | 13.74 | 0.85 | 1.66 | 264 | 3.69 | 0.66 | 0.04 | 0.08 | 264 |
| No.bb.17229 | 1932 | 306.19 | 65.65 | 16.13 | 1.18 | 2.32 | 186 | 3.01 | 0.64 | 0.05 | 0.09 | 186 |
| No.bb.18328 | 1934 | 306.46 | 67.24 | 14.92 | 1.11 | 2.18 | 180 | 3.69 | 1.08 | 0.08 | 0.16 | 180 |
| No.bb.21151 | 1936 | 306.76 | 70.57 | 14.53 | 1.08 | 2.12 | 180 | 4.30 | 0.89 | 0.07 | 0.13 | 180 |
| No.SFN30887 | 1936 | 306.76 | 71.54 | 15.12 | 0.84 | 1.65 | 322 | 4.01 | 0.99 | 0.05 | 0.11 | 322 |
| No.61064 | 1947 | 309.82 | 58.65 | 14.54 | 1.24 | 2.43 | 137 | 3.17 | 1.02 | 0.09 | 0.17 | 137 |
| No.57330 | 1947 | 309.82 | 71.56 | 15.61 | 1.42 | 2.78 | 121 | 4.03 | 0.89 | 0.08 | 0.16 | 121 |
| No.57329 | 1947 | 309.82 | 69.90 | 16.33 | 1.23 | 2.41 | 177 | 3.62 | 0.77 | 0.06 | 0.11 | 177 |
| No.55897 | 1947 | 309.82 | 72.49 | 14.95 | 1.35 | 2.65 | 122 | 3.77 | 1.04 | 0.09 | 0.18 | 122 |
| No.40798 | 1955 | 313.73 | 49.60 | 14.31 | 0.82 | 1.60 | 306 | 3.37 | 0.96 | 0.05 | 0.11 | 306 |
| No.KEP80548 | 1965 | 320.04 | 60.00 | 14.53 | 0.78 | 1.53 | 346 | 3.25 | 0.84 | 0.05 | 0.09 | 346 |
| No.FRI33343 | 1987 | 348.98 | 55.61 | 12.53 | 0.58 | 1.13 | 475 | 3.28 | 0.88 | 0.04 | 0.08 | 475 |
| Mean | — | — | 66.14 | 14.77 | 1.04 | 2.08 | 235 | 3.60 | 0.89 | 0.06 | 0.12 | 235 |

Note: *x*—mean; σ —standard deviation; s.e. —standard error of mean; n— numbers of photos counts (40 \times); t*s.e.— 95% confidence interval.

754

755 Table 5. Summary of stomatal parameters from modern *Nageia motleyi* (Parl.) De Laub (Kouwenberg et al., 2003).

| Collection number | Collection date | CO ₂ (ppmv) | SNL | SDL | TSDL | n |
|-------------------|-----------------|------------------------|-------|--------|---------|-----|
| No.2649 | 1868 | 289.23 | 11.64 | 394.38 | 1455.10 | 264 |
| No.bb.17229 | 1932 | 306.19 | 9.19 | 337.98 | 1280.12 | 186 |
| No.bb.18328 | 1934 | 306.46 | 8.71 | 378.92 | 1277.63 | 180 |
| No.bb.21151 | 1936 | 306.76 | 9.62 | 376.93 | 1517.21 | 180 |
| No.SFN30887 | 1936 | 306.76 | 10.55 | 325.08 | 735.38 | 240 |
| No.61064 | 1947 | 309.82 | 8.19 | 282.04 | 1200.66 | 133 |
| No.57330 | 1947 | 309.82 | 9.67 | 397.83 | 1397.33 | 119 |
| No.57329 | 1947 | 309.82 | 10.13 | 350.98 | 1672.50 | 176 |
| No.55897 | 1947 | 309.82 | 10.48 | 379.06 | 1486.13 | 122 |
| No.40798 | 1955 | 313.73 | 10.29 | 175.14 | 933.85 | 305 |
| No.KEP80548 | 1965 | 320.04 | 9.36 | 266.16 | 585.72 | 263 |
| No.FRI33343 | 1987 | 348.98 | 9.84 | 252.20 | 1181.51 | 125 |
| Mean | – | – | 9.81 | 326.39 | 1226.93 | 191 |

756

757

758

759 Table 6. Summary of stomatal parameters of the adaxial surface of fossil *Nageia* and pCO₂ [*C_f*] estimates results.

| Species | Age | SD (mm ⁻²) | | | | SI (%) | | | | SR | | pCO ₂ (ppmv) | | <i>C_f</i> (ppmv) | |
|-----------|-------------|------------------------|----------|------|-----|----------|----------|------|-----|----------|-------|-------------------------|-------|-----------------------------|-------|
| | | <i>x</i> | σ | s.e. | n | <i>x</i> | σ | s.e. | n | <i>x</i> | t*s.e | <i>x</i> | t*s.e | <i>x</i> | t*s.e |
| MMJ1-001 | Late Eocene | 52.5 | 17.1 | 3.1 | 30 | 2.08 | 0.7 | 0.1 | 30 | 1.35 | 0.19 | 333.6 | 13.9 | 412.1 | 62.0 |
| MMJ2-003 | Late Eocene | 42.3 | 12.9 | 2.4 | 30 | 1.80 | 0.6 | 0.1 | 30 | 1.75 | 0.39 | 356.8 | 10.5 | 536.1 | 126.2 |
| MMJ2-004 | Late Eocene | 39.9 | 13.6 | 2.5 | 30 | 1.66 | 0.6 | 0.1 | 30 | 1.81 | 0.32 | 362.4 | 11.0 | 554.3 | 101.9 |
| MMJ3-003a | Late Eocene | 43.2 | 17.7 | 3.2 | 30 | 1.67 | 0.7 | 0.1 | 30 | 1.84 | 0.43 | 354.8 | 14.4 | 564.6 | 135.7 |
| Mean | Late Eocene | 44.5 | 16.3 | 1.5 | 120 | 1.80 | 0.7 | 0.1 | 120 | 1.69 | 0.18 | 351.9 | 6.6 | 516.8 | 56.5 |

Note: *x*—mean; σ —standard deviation; s.e. —standard error of mean; n— numbers of photos counts (400×); t*s.e.— 95% confidence interval. pCO₂— the result based the regression approach; *C_f*— the result based on the stomatal method.

760

761

762 Table 7. Summary of stomatal parameters of the abaxial surface of fossil *Nageia* and pCO₂ [*C_f*] estimates results.

| Species | Age | SD (mm ⁻²) | | | | SI (%) | | | | SR | | pCO ₂ (ppmv) | | <i>C_f</i> (ppmv) | |
|-----------|-------------|------------------------|----------|------|-----|----------|----------|------|-----|----------|-------|-------------------------|-------|-----------------------------|-------|
| | | <i>x</i> | σ | s.e. | n | <i>x</i> | σ | s.e. | n | <i>x</i> | t*s.e | <i>x</i> | t*s.e | <i>x</i> | t*s.e |
| MMJ1-001 | Late Eocene | 47.7 | 17.7 | 3.2 | 30 | 2.11 | 0.8 | 0.2 | 30 | 1.66 | 0.23 | 368.6 | 16.2 | 515.6 | 72.3 |
| MMJ2-003 | Late Eocene | 50.9 | 18.3 | 3.3 | 30 | 2.12 | 0.8 | 0.1 | 30 | 1.57 | 0.23 | 360.9 | 16.6 | 486.0 | 70.7 |
| MMJ2-004 | Late Eocene | 48.2 | 15.8 | 2.9 | 30 | 2.14 | 0.7 | 0.1 | 30 | 1.63 | 0.25 | 367.4 | 14.5 | 504.6 | 77.3 |
| MMJ3-003a | Late Eocene | 48.9 | 12.6 | 2.7 | 22 | 1.85 | 0.5 | 0.1 | 22 | 1.52 | 0.19 | 365.4 | 13.5 | 472.3 | 59.0 |
| Mean | Late Eocene | 48.9 | 16.2 | 1.5 | 112 | 2.07 | 0.7 | 0.1 | 112 | 1.60 | 0.11 | 365.6 | 7.6 | 496.1 | 35.7 |

Note: *x*—mean; σ —standard deviation; s.e. —standard error of mean; n— numbers of photos counts (400×); t*s.e.— 95% confidence interval. pCO₂— the result based the regression approach; *C_f*— the result based on the stomatal method.

763

764 Table 8. Summary of stomatal parameters of the combined data of the adaxial and abaxial surfaces of fossil *Nageia* and pCO₂ [*C*_(f)] estimates
 765 results.

| Species | Age | SD (mm ⁻²) | | | | SI (%) | | | | SR | | pCO ₂ (ppmv) | | <i>C</i> _(f) (ppmv) | |
|-----------|-------------|------------------------|----------|------|-----|----------|----------|------|-----|----------|-------|-------------------------|-------|--------------------------------|-------|
| | | <i>x</i> | σ | s.e. | n | <i>x</i> | σ | s.e. | n | <i>x</i> | t*s.e | <i>x</i> | t*s.e | <i>x</i> | t*s.e |
| MMJ1-001 | Late Eocene | 50.1 | 17.5 | 2.3 | 60 | 2.09 | 0.8 | 0.1 | 60 | 1.50 | 0.15 | 349.7 | 10.6 | 471.2 | 47.8 |
| MMJ2-003 | Late Eocene | 46.5 | 16.3 | 2.1 | 60 | 1.96 | 0.7 | 0.1 | 60 | 1.67 | 0.24 | 358.3 | 9.8 | 524.1 | 75.7 |
| MMJ2-004 | Late Eocene | 44.0 | 15.8 | 2.0 | 60 | 1.90 | 0.7 | 0.1 | 60 | 1.73 | 0.17 | 364.3 | 9.5 | 542.9 | 52.6 |
| MMJ3-003a | Late Eocene | 45.6 | 16.1 | 2.2 | 52 | 1.75 | 0.6 | 0.1 | 52 | 1.73 | 0.28 | 360.5 | 10.4 | 544.6 | 88.3 |
| Mean | Late Eocene | 46.6 | 16.4 | 1.1 | 232 | 1.93 | 0.7 | 0.1 | 232 | 1.66 | 0.11 | 358.1 | 5.0 | 519.9 | 35.0 |

Note: *x*—mean; σ —standard deviation; s.e. —standard error of mean; n— numbers of photos counts (400×); t*s.e.— 95% confidence interval. pCO₂— the result based the regression approach; *C*_(f)— the result based on the stomatal method.

766

767 Table 9. pCO₂ estimates proxies and corresponding references.

| Proxies | References |
|---------------|-------------------------------------------------------------------------------------------------------------------------------------------------------------------------------------------------------------------------------------------------------------------------------------------------|
| Boron | Pearson et al., 2009; Seki et al., 2010 |
| B/Ca | Tripathi et al., 2009 |
| Phytoplankton | Freeman and Hayes, 1992; Stott, 1992; Pagani et al., 1999, 2005; Henderiks and Pagani, 2008; Seki et al., 2010 |
| Nahcolite | Lowenstein and Demicco, 2006 |
| Liverworts | Fletcher et al., 2008 |
| Paleosols | Cerling, 1992; Koch et al., 1992; Ekart et al., 1999; Royer et al., 2001; Nordt et al., 2002; Retallack, 2009b; Huang et al. 2013 |
| Stomata | Van der Burgh et al., 1993; Kürschner et al., 1996, 2001, 2008; McElwain, 1998; Royer et al., 2001, 2003; Greenwood et al., 2003; Beerling et al., 2009; Retallack, 2009a; Smith et al., 2010; Doria et al., 2011; Roth-Nebelsick et al., 2012; 2014; Grein et al., 2013; Maxbauer et al., 2014 |

768